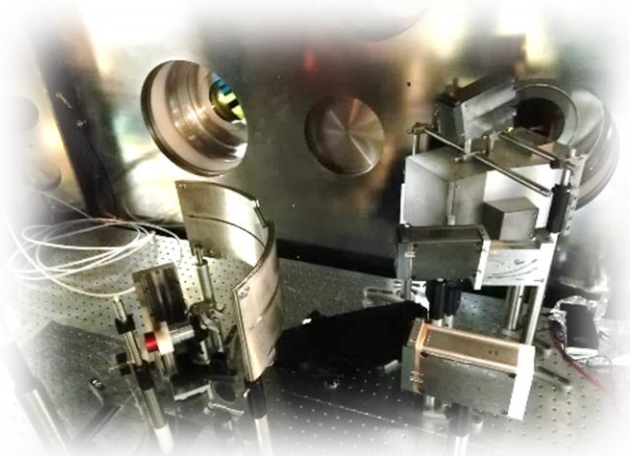
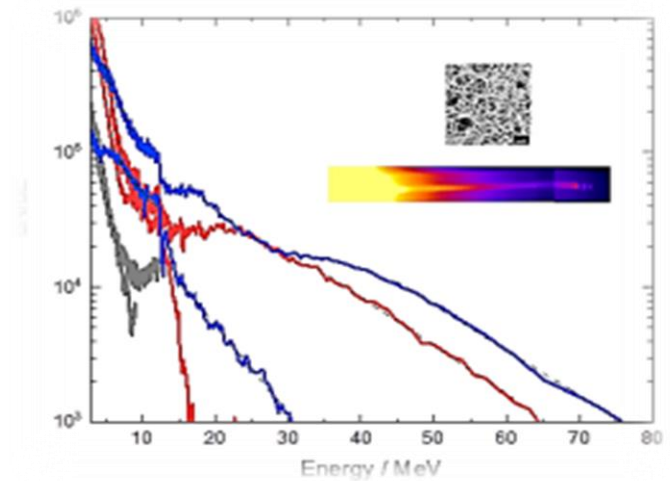


High current well-directed beams of super-ponderomotive electrons for laser driven nuclear physics applications.

«Ускорение частиц в плазме и лазерно-плазменная физика экстремального света»
онлайн-семинар, 16.10.2020



Olga Rosmej



GSI Darmstadt,
Plasma Physics Group, IAP, GU-Frankfurt
Helmholtz Research Academy Hessen for FAIR

Plasma Physics, HED-research:

ultra-intense betatron, THz and gamma-sources,

Nuclear Physics:

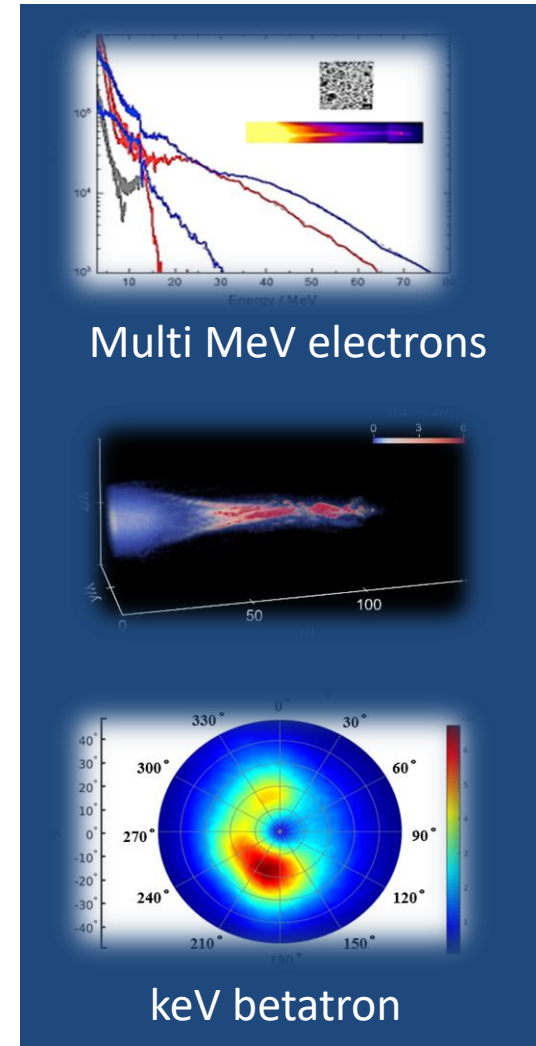
high fluence/ flux gamma and neutron sources,
high yield (p,xn), (g,xn) nuclear reactions in GDR region
theranostic relevant radio-isotopes.

Biophysics:

high flux ionizing radiation (e^- , γ) for investigation
of the FLASH-effect in the tumor therapy.

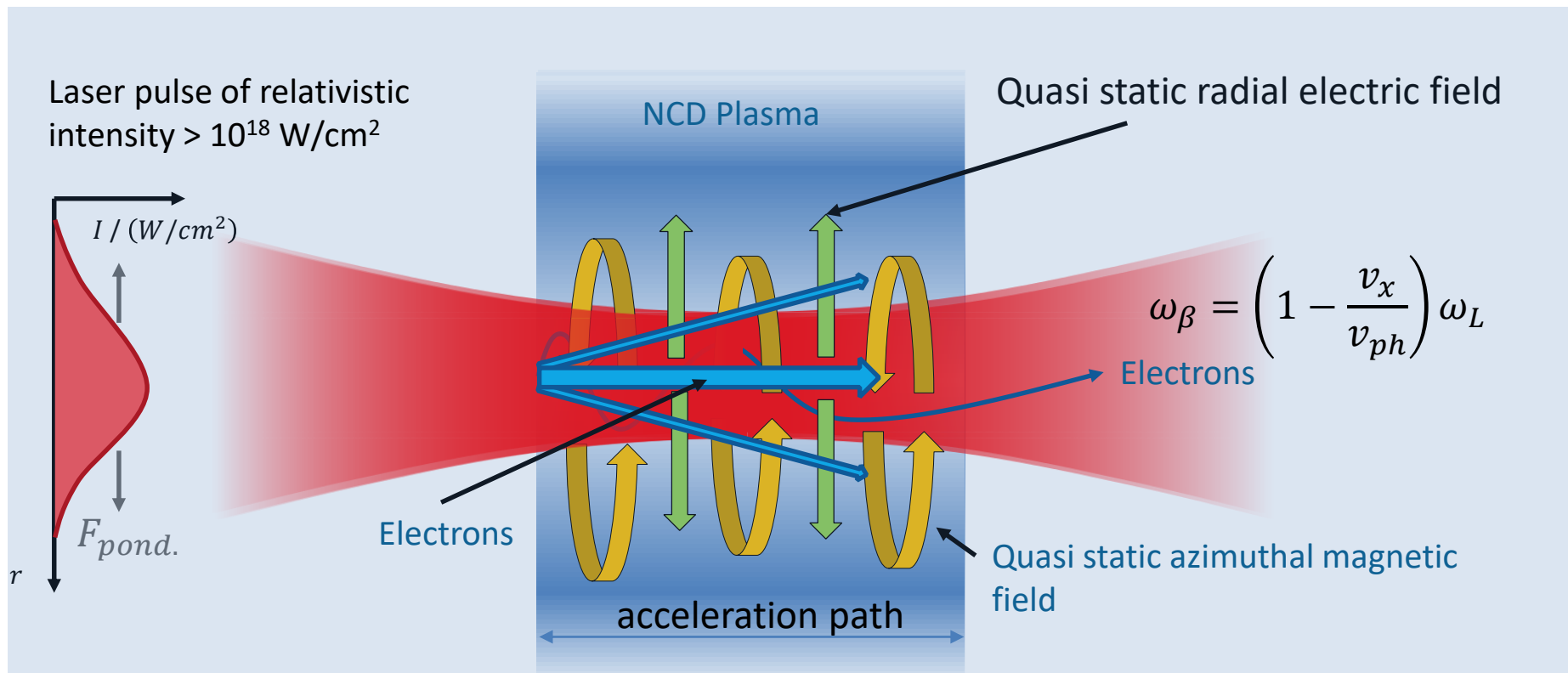
Collaboration: Experiment-PIC-GEANT4

GSI-Darmstadt (PP, BP); GU-Frankfurt;
HH-Düsseldorf; FS, HI-Jena; JIHT Moscow;
LPI-Moscow; ITEP-Moscow



ACCELERATION OF ELECTRONS IN PLASMA OF NEAR CRITICAL DENSITY

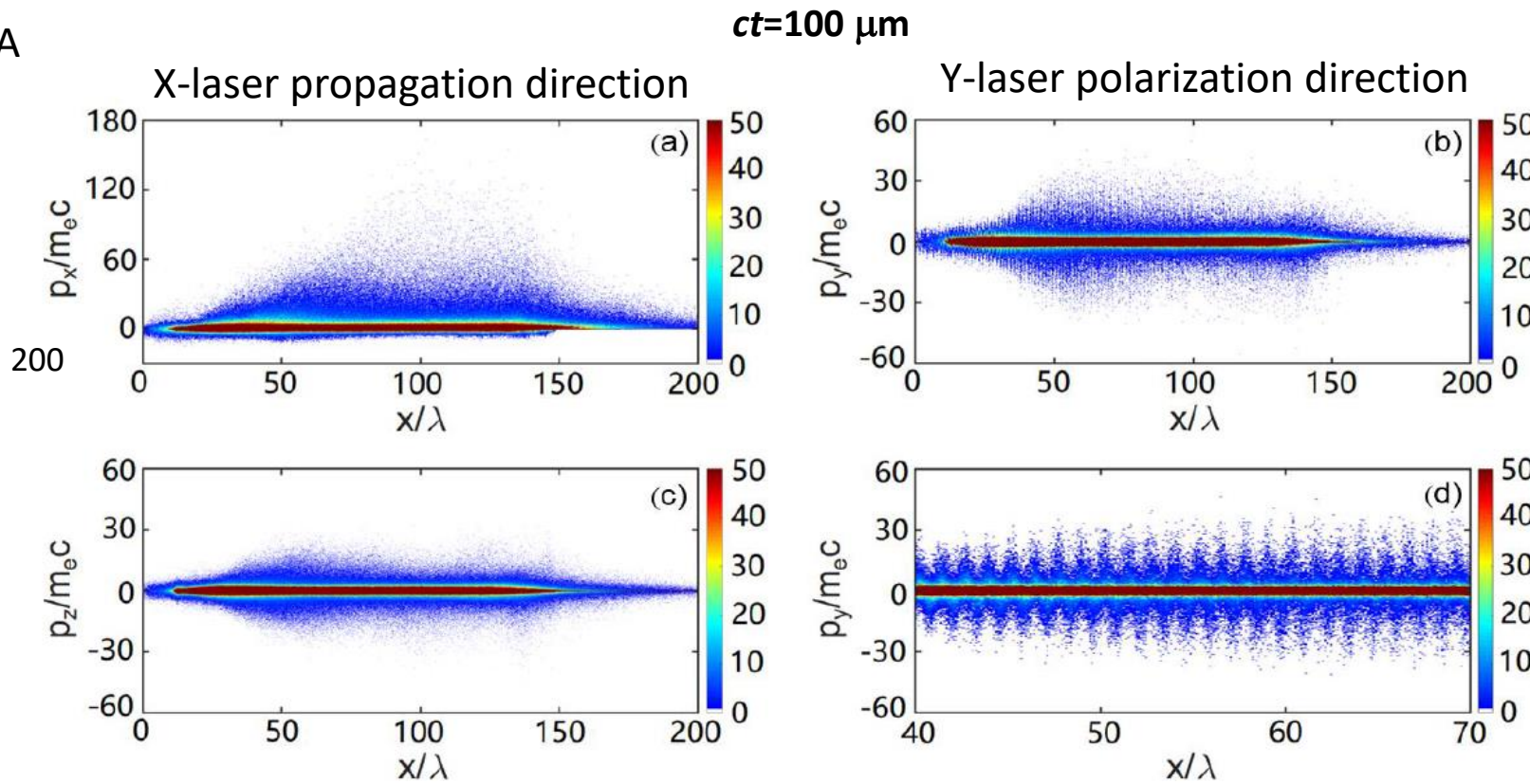
Direct laser acceleration of relativistic electrons at betatron resonance
A. Pukhov, Z.-M. Sheng, and J. Meyer-ter-Vehn, V6, N7, PoP 1999



- self-focusing : $P_L > P_c = 17 \text{ GW} \times n_c / n_e$ (high aspect ration channel)
- generation of quasi-static radial E-field that has a pinching polarity for electrons.
- self-generated quasi-static B azimuthal that traps electrons in the plasma channel.

PHASE SPASE OF ACCELERATED ELECTRONS

DLA

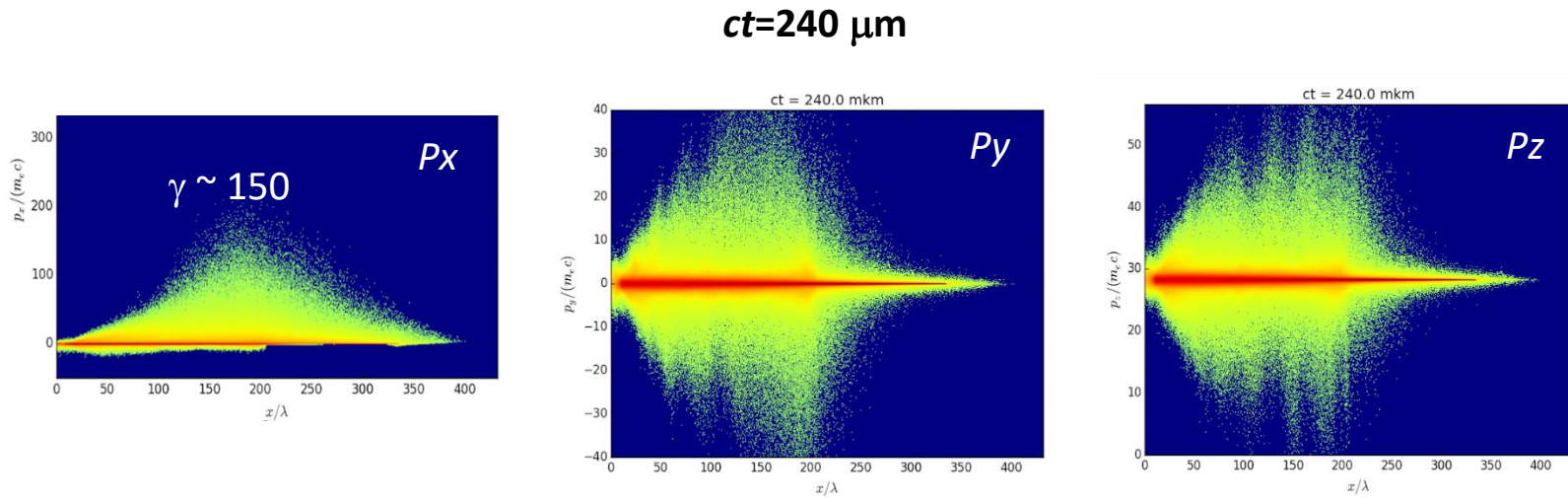


Snapshots of the electron phase space at $ct=100\mu\text{m}$ after the laser pulse peak intensity arrived at the left plasma boundary: (a) momentum p_x vs x ; (b) momentum p_y vs x ; (c) momentum p_z vs x ; (d) zoomed part of momentum p_y vs x in the range $x/\lambda = [40, 70]$.

Color panels present a number of pseudo-electrons in simulations.

3D-PIC simulations X. Shen

At later times, stochastic heating starts to play a major role



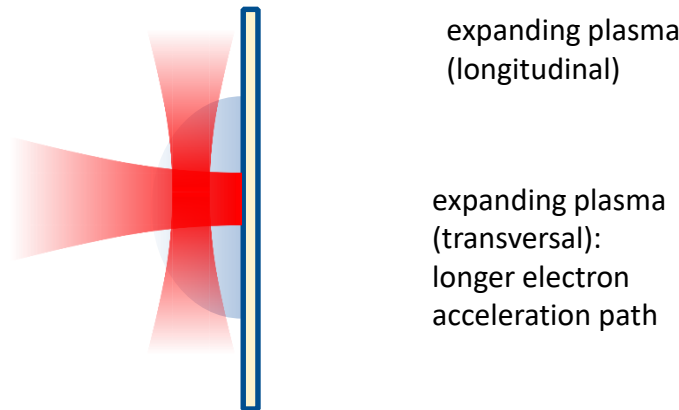
stochastic feature ($P_z \sim P_y$)

3D-PIC simulations V. Popov

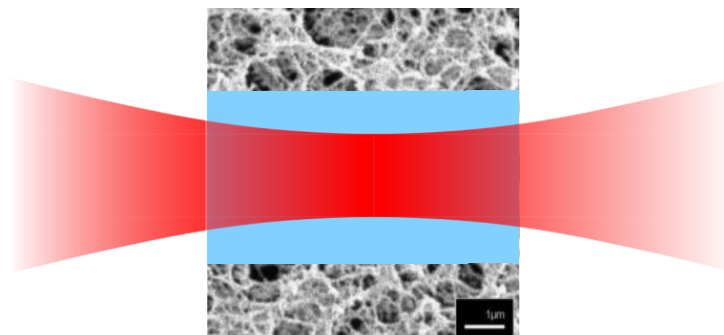
GENERATION OF PLASMA WITH NEAR CRITICAL ELECTRON DENSITY

- Critical density $n_c(1054 \text{ nm}) = \frac{\epsilon_0 m_e}{e^2} \omega_L^2 = 10^{21} \text{ cm}^{-3}$

→ Foil target:

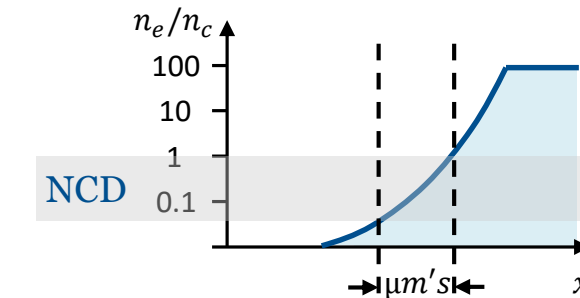


→ Foam target:

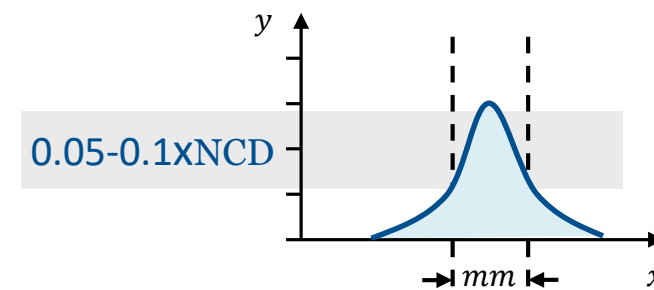


CHO-Foams (Triacetatecellulose: $C_{12}H_{16}O_8$):
300 – 500 μm , 2 mg/cm^3

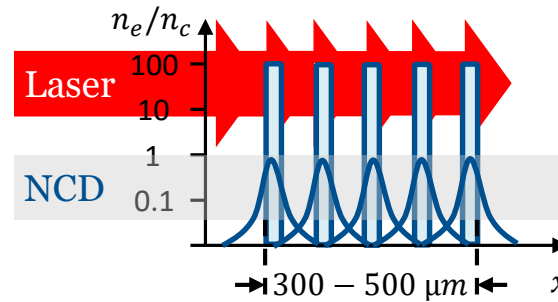
supersonic ionization $v = 500 \mu\text{m}/2\text{ns}$



Pukhov, A., et al. *Physics of Plasmas* 6.7 (1999)



Willingale, L., et al. *New Journal of Physics* 15.2 (2013): 025023.

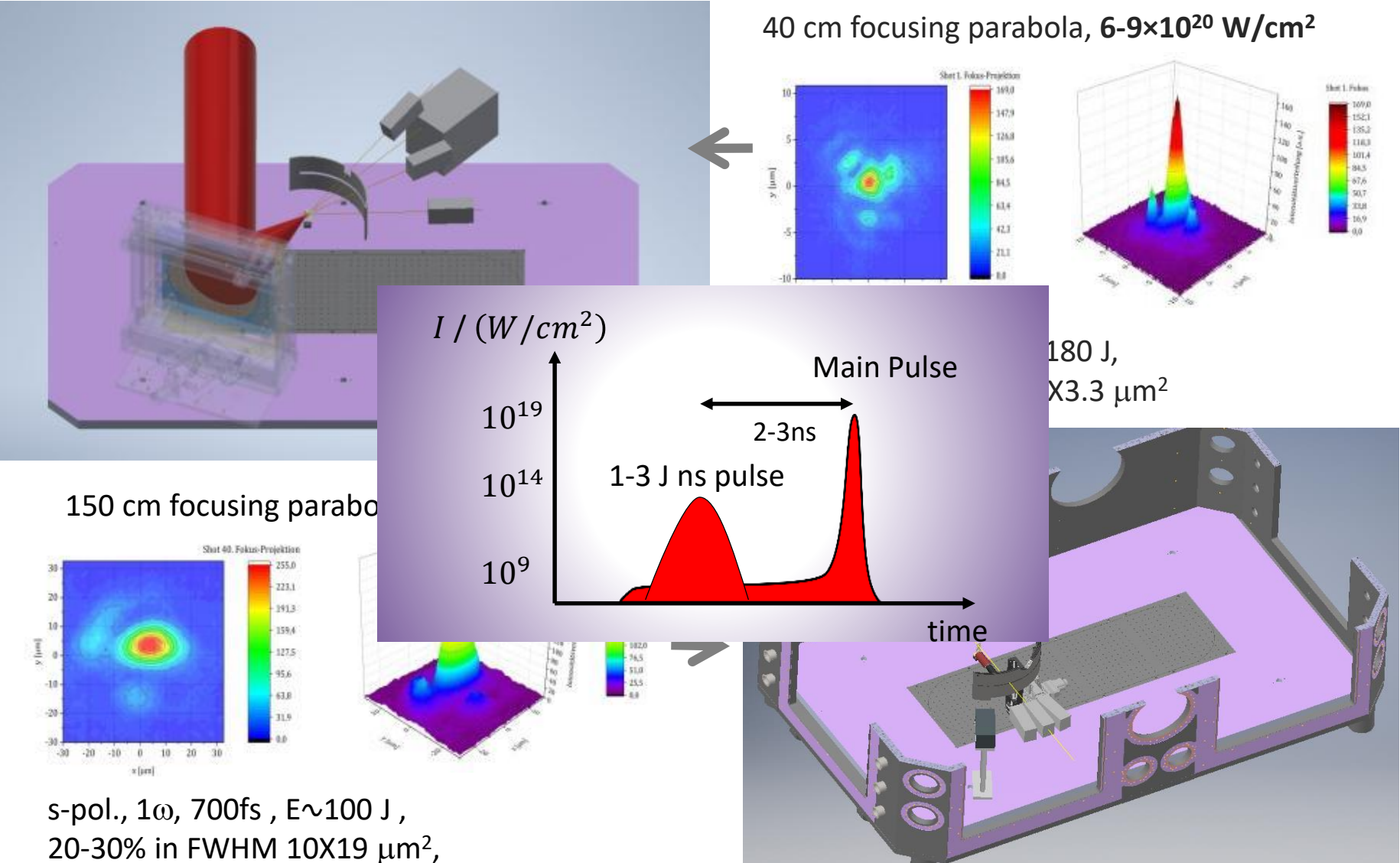


Rosmej, O et al 2019 *New J. Phys.* **21** 043044

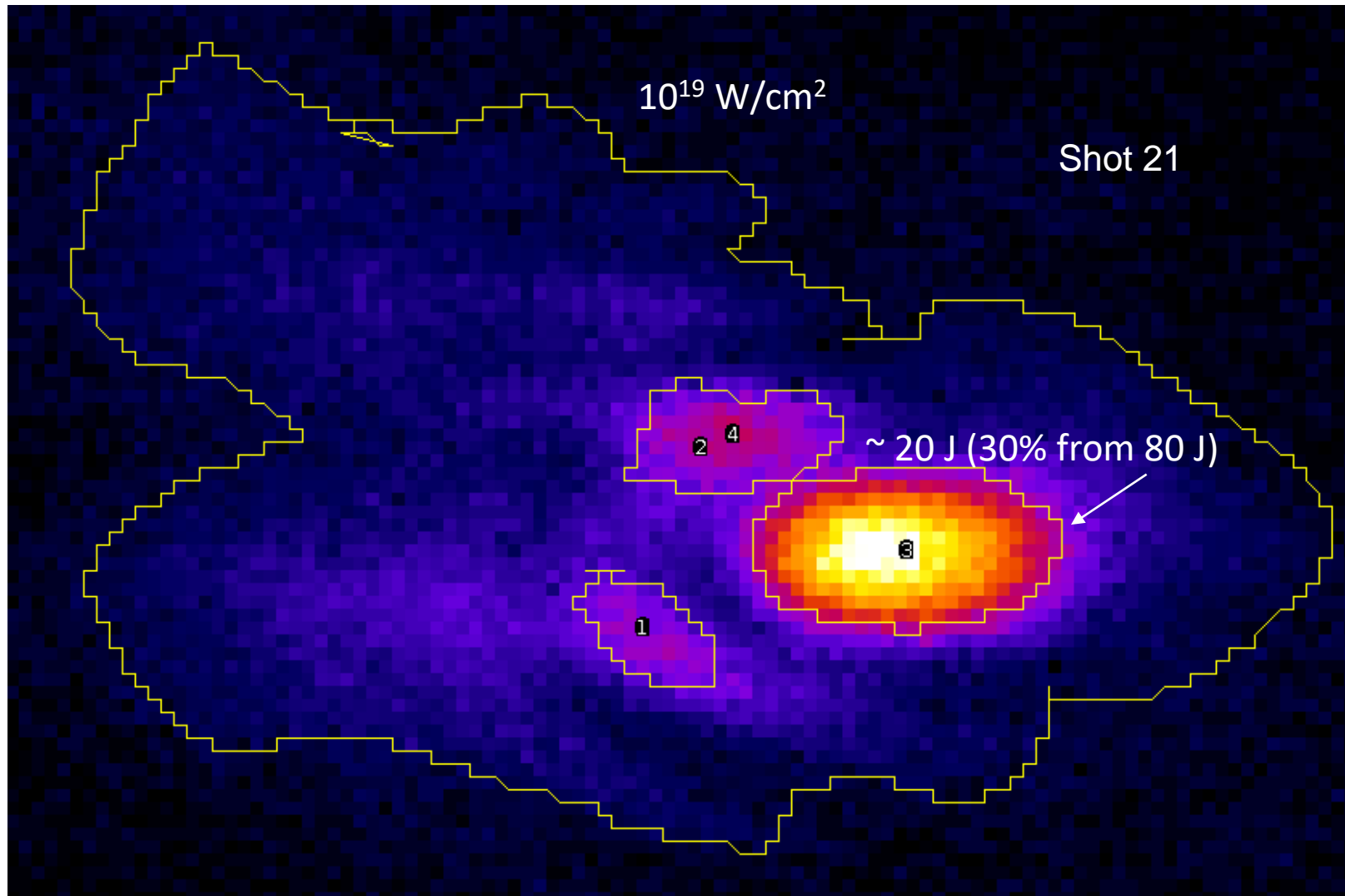
SET-UPS FOR DIFFERENT PHELIX-LASER INTENSITIES

1ω Nd:glass

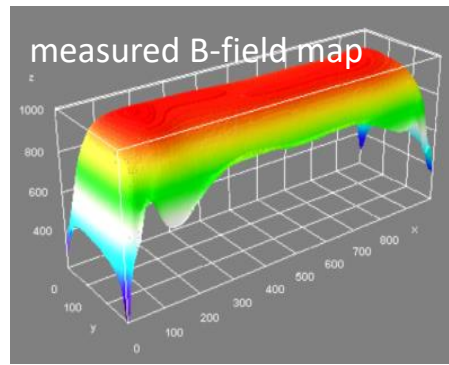
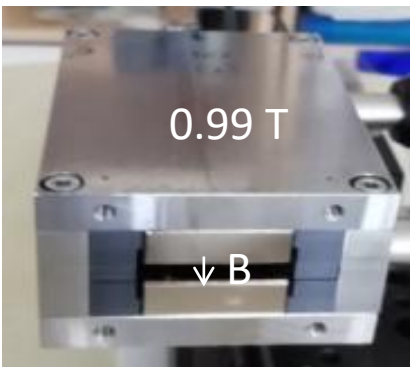
Experiments were performed at 10^{21}W/cm^2 and 10^{19}W/cm^2



DISTRIBUTION OF LASER ENERGY IN THE FOCAL SPOT

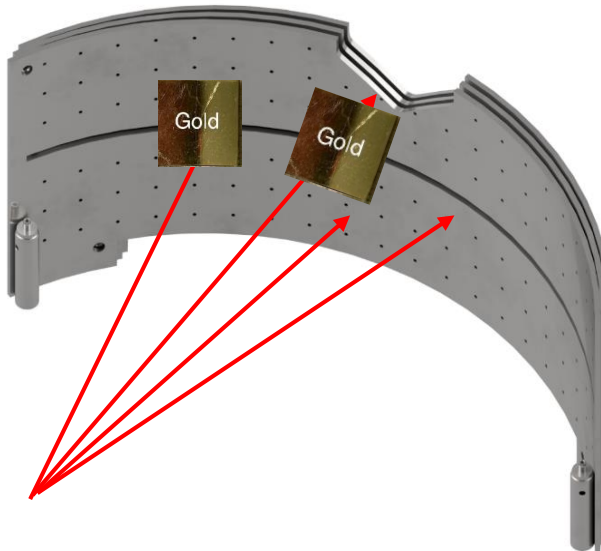


Electron spectrometer:
electron energy distribution



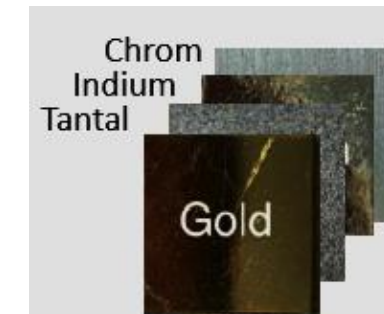
Static magnets, $B=0.99\text{T}$
2% energy resolution up to 100 MeV
Detector: calibrated imaging plates
-> absolute number of electrons

Cylinder diagnostic:
electron angular distribution

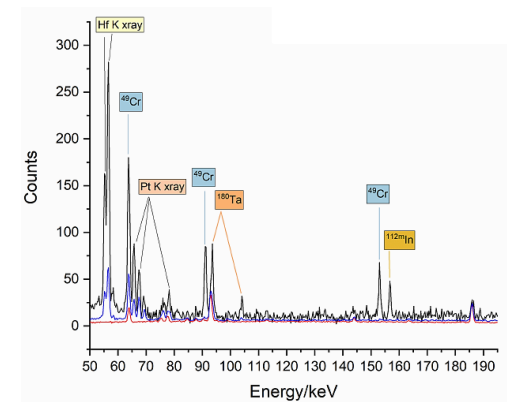


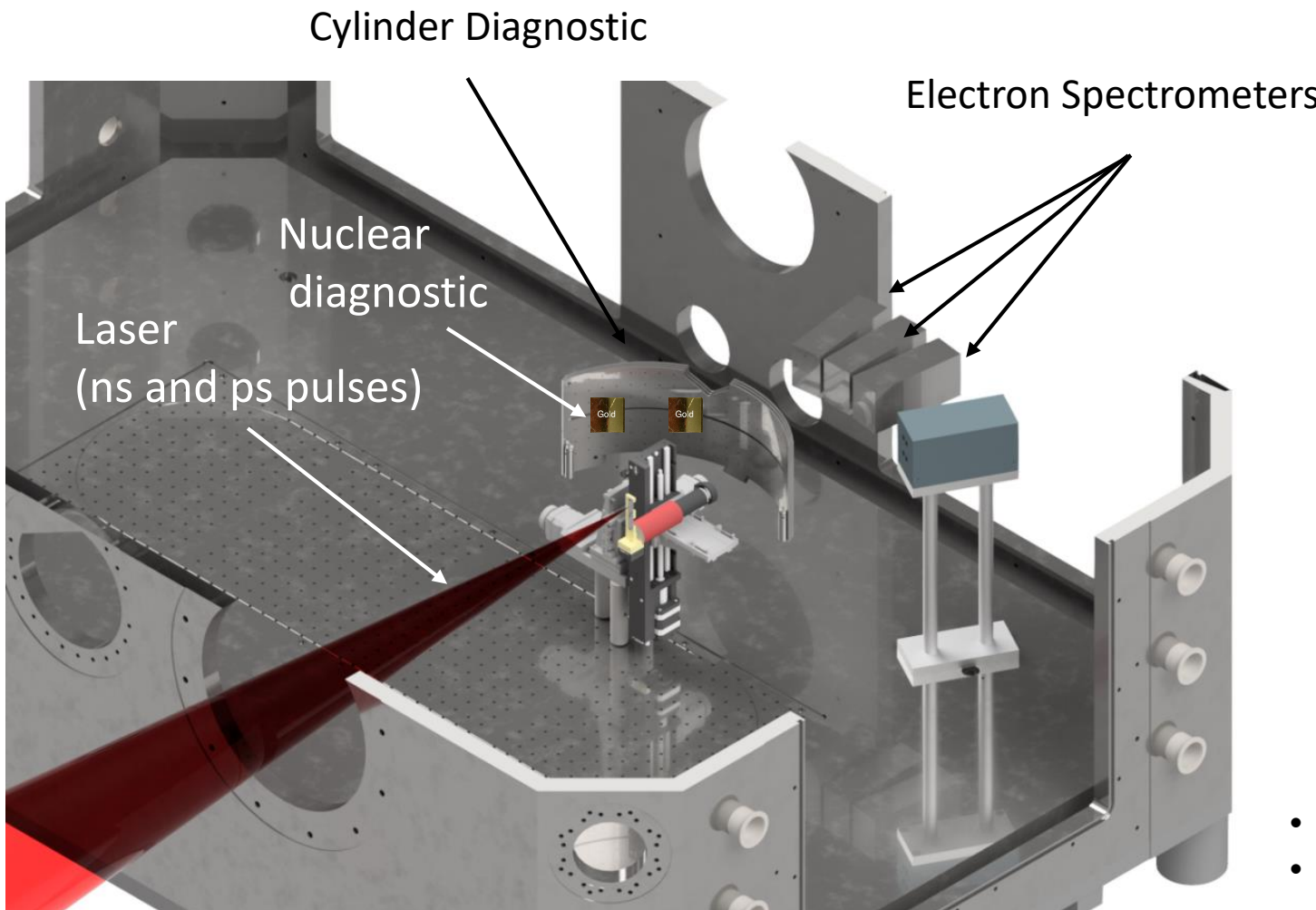
3 cylinders, 3mm steel each
 $R=200\text{mm}$
Detector: imaging plates

Nuclear diagnostic:
 γ , neutron fluences



Ge-detector:
isotope type and number





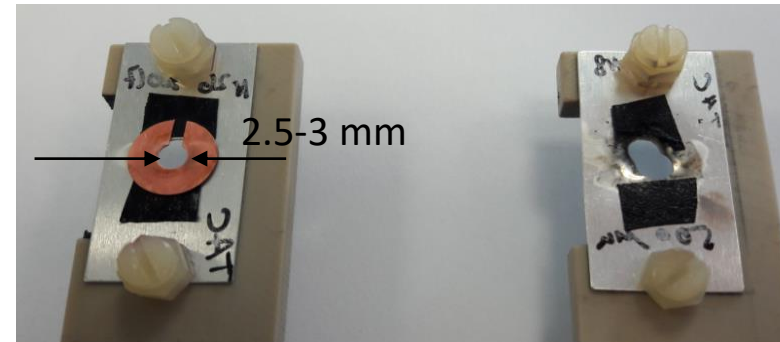
Target-Holder

- $10 \mu\text{m}$ Ti, Au-foils
- 1-2mm Au, W plates
- CHO- foams
- combination

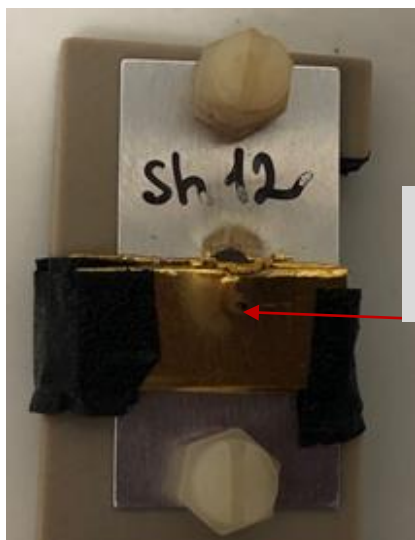
NCD plasma: low density polymer foams $\rho=2 \text{ mg/cc}$ ($1.7 \times 10^{20} \text{ at/cm}^3$)
 300-500 μm thickness, fully ionized ($Z_{\text{mean}}=4.2$) $\rightarrow n_e = 0.65 \times 10^{21} \text{ cm}^{-3}$

TARGETS AFTER INTERACTION

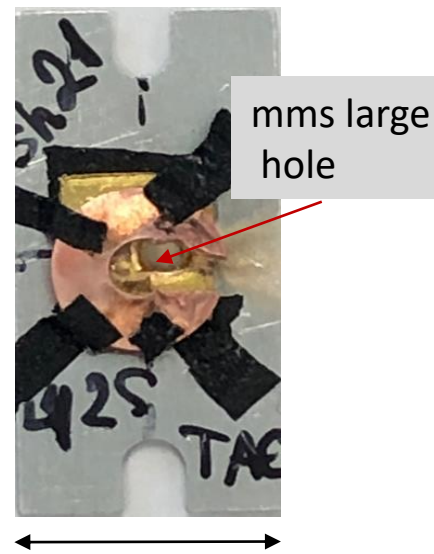
500 μm 2 mg/cc foam =
700 nm 1.4 g/cc polymer foil



shot 12:
 10^{21}W/cm^2 : 40J, d=3 μm
(1+1)mm Au-radiator



shot 21:
 10^{19}W/cm^2 : 20J d=15 μm
Foam+ 1mm Au



Sh. 28
500 μm foam

shot 28:
 10^{19}W/cm^2 : 20J d=15 μm
Foam+ 0.1mm Pb



N. Borisenko, LPI

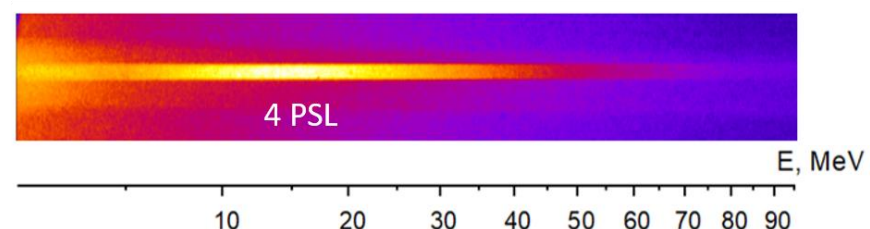
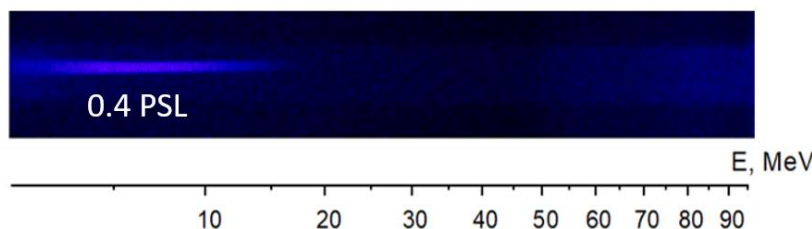
ENERGY AND ANGULAR DISTRIBUTION of MeV-ELECTRONS

Highly energetic and well directed electron beam ($\gamma > 10$) generated in NCD plasma

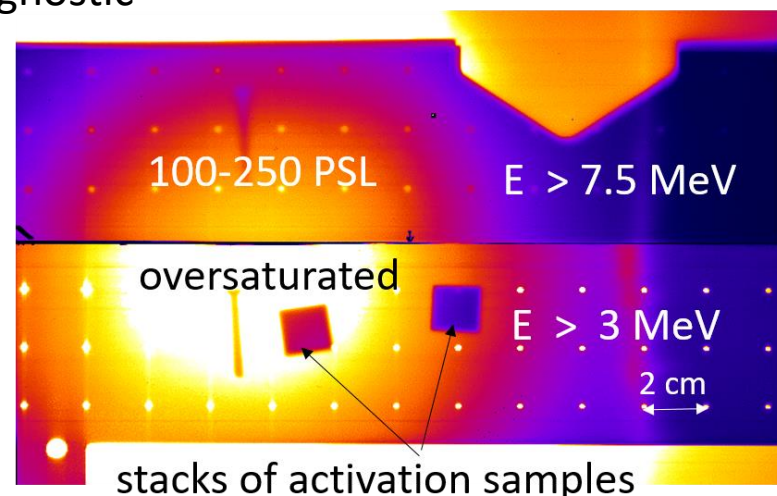
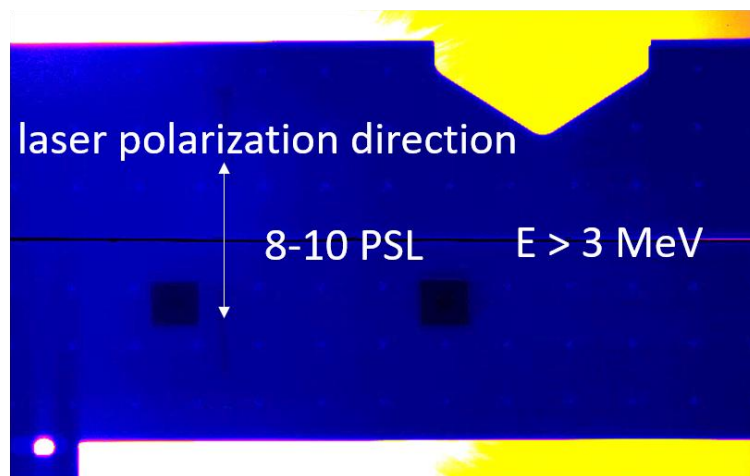
Shot 40: 700 fs, 10^{19} W/cm²
Target: Au foil 10 um

Shot 42: 700 fs, 10^{19} W/cm²
Target: 325 um TAC + Au foil 10 um

electron spectra at 0° to laser axis



cylinder diagnostic

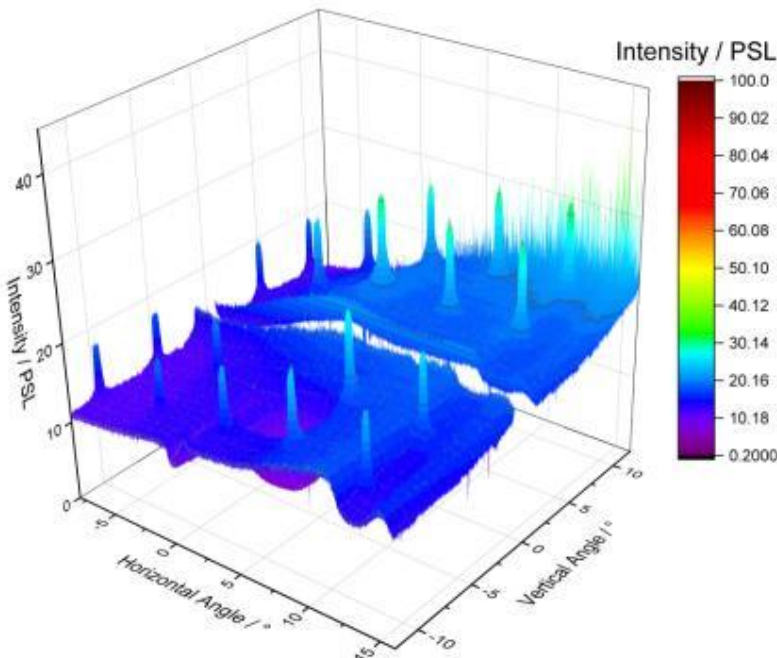


ANGULAR DISTRIBUTION OF RELATIVISTIC ELECTRONS

Well directed electron beam ($\gamma > 10$) generated in foams

Shot 40: 700 fs, 10^{19} W/cm²
Target: Au foil 10 um

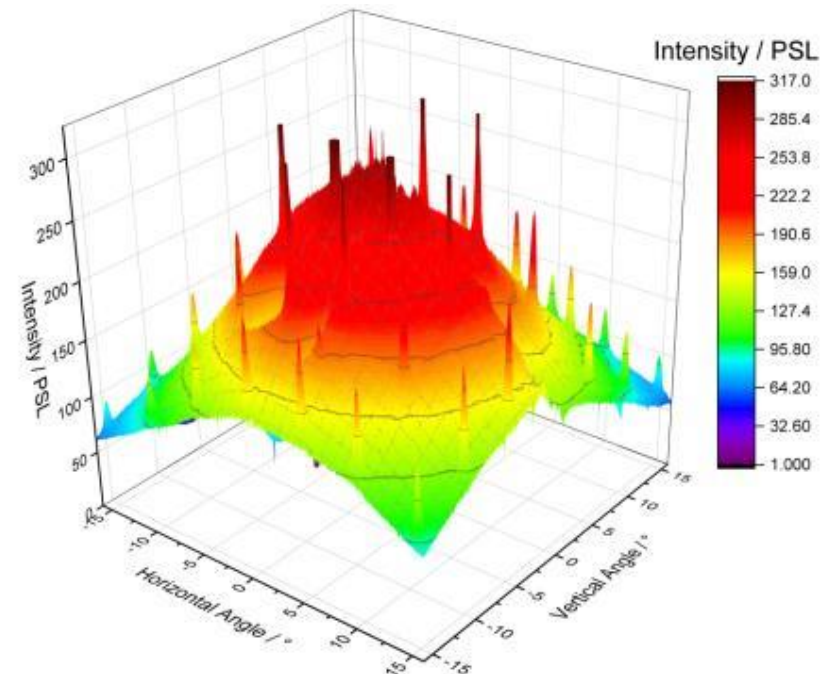
no directionality



low IP signal,

Shot 42: 700 fs, 10^{19} W/cm²
Target: 325 um 2 mg/cc TAC+ Au foil 10 um

$\frac{1}{2} \theta$ at FWHM $\leq 13^\circ$

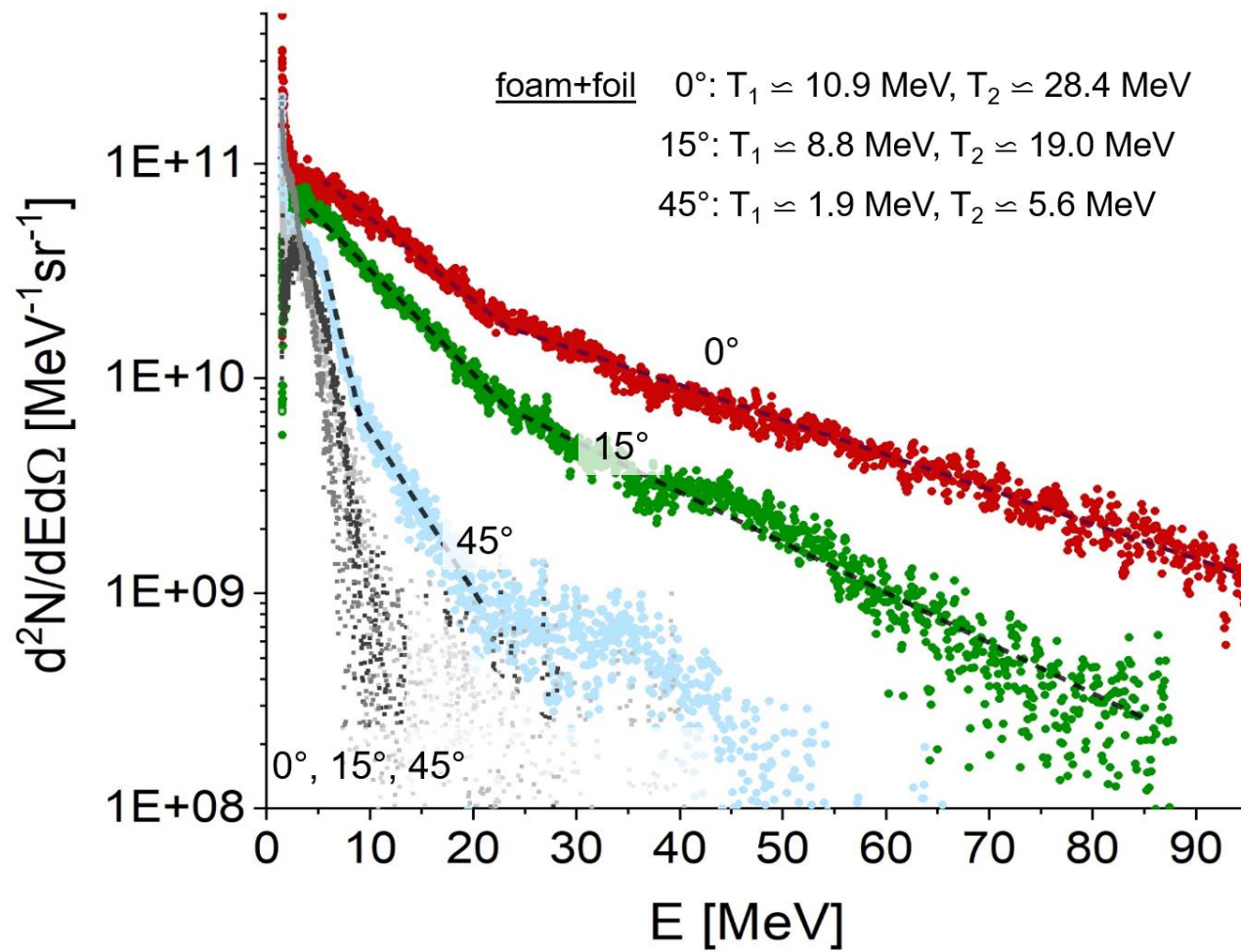


more than 30 times increase of the IP signal,

S. Zähter, GSI

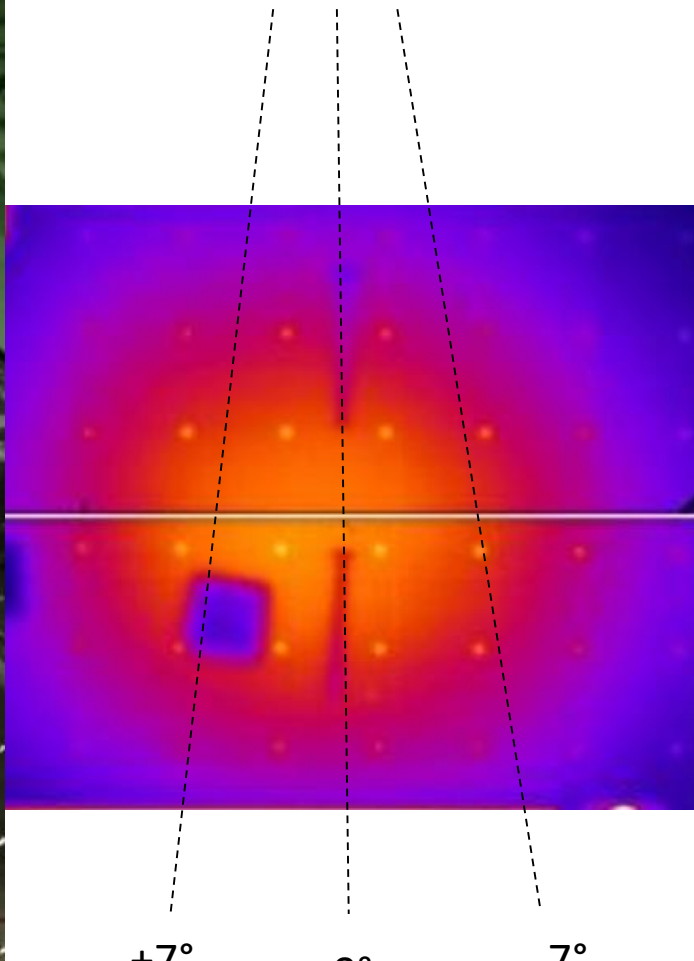
ENERGY DISTRIBUTION OF SUPER-PONDEROMOTIVE ELECTRONS

700 fs, $E_{FWHM} = 20 \text{ J}$, 10^{19} W/cm^2
target: foam + foil



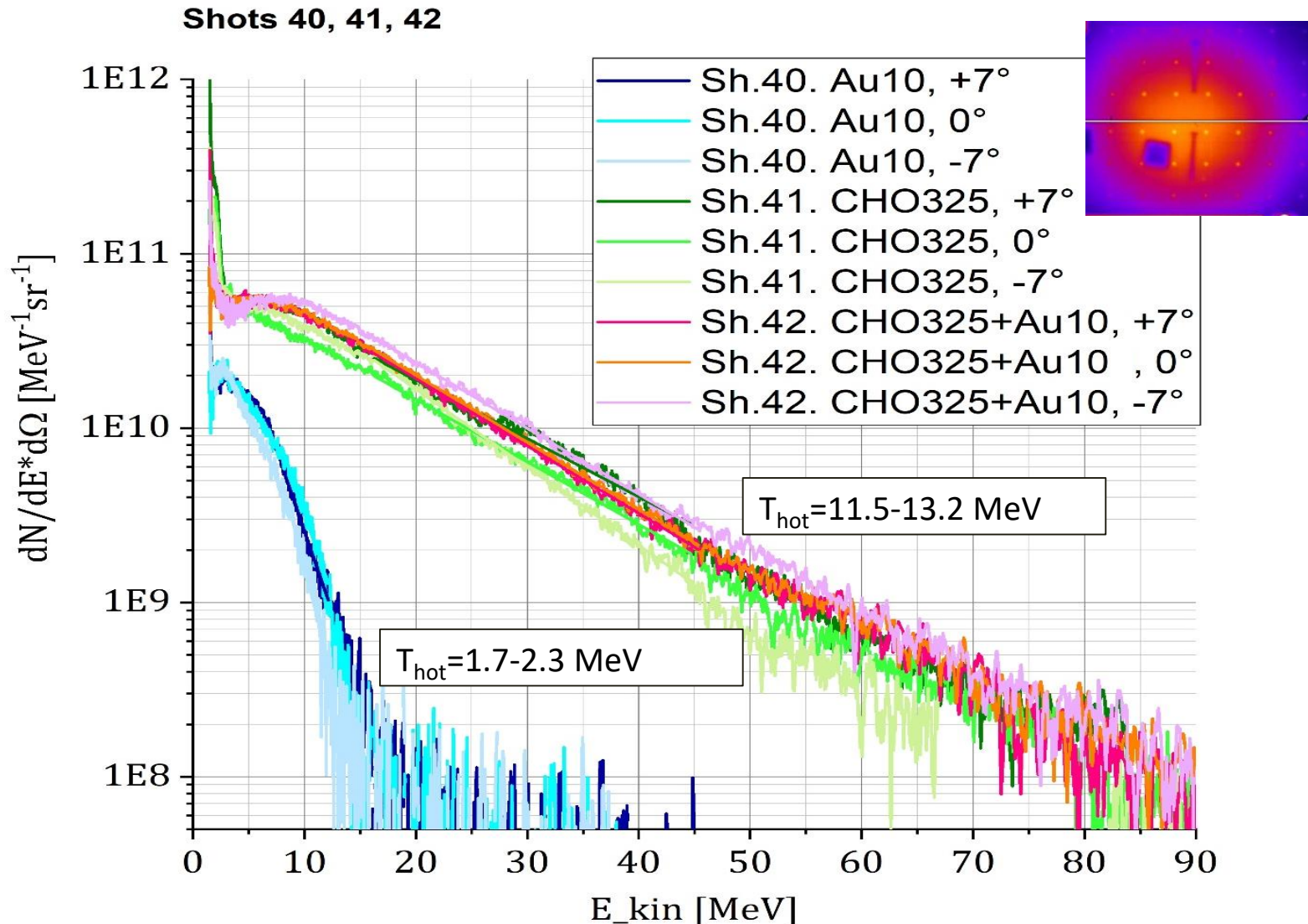
M. Gyrdymov, Frankfurt University

ENERGY AND NUMBER OF MeV-ELECTRONS INSIDE DIVERGENCE CONE



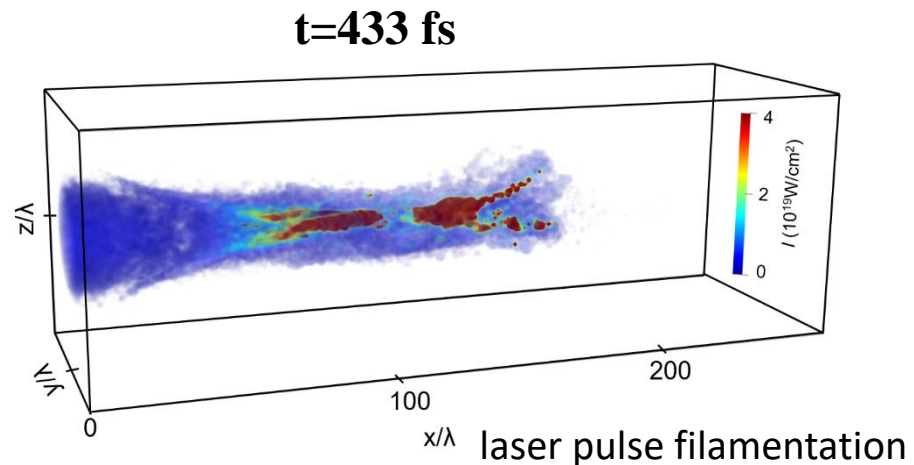
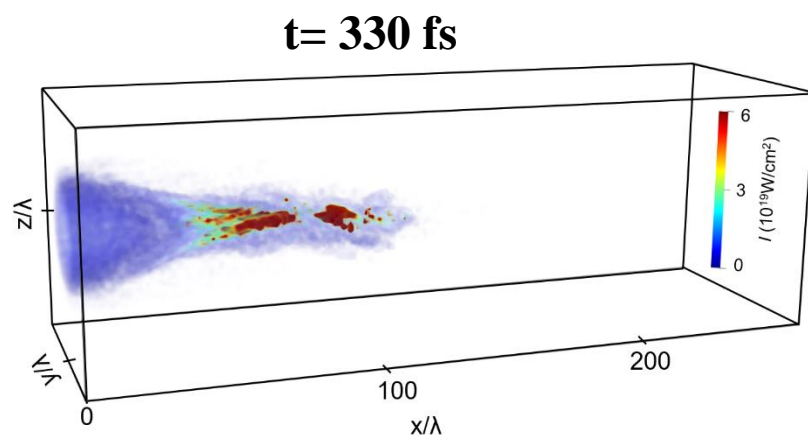
M. Gyrdymov, Frankfurt University

ENERGY AND NUMBER OF MeV-ELECTRONS INSIDE DIVERGENCE CONE



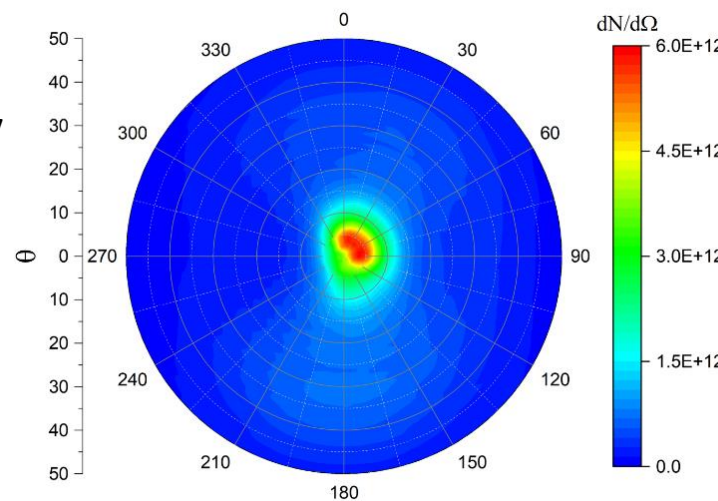
FULL 3D-PIC SIMULATIONS

3D view of the laser intensity distribution



**Angular distribution
of electrons with $E > 7$ MeV**

$\frac{1}{2} \theta$ at FWHM $\sim 10^\circ$
(experiment $< 13^\circ$)

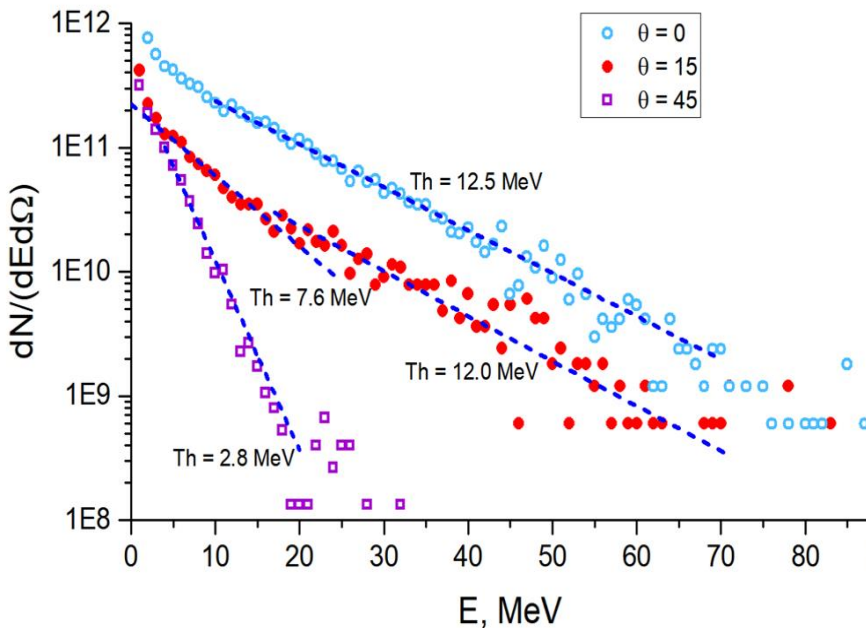


A. Pukhov, N. Andreev,
X. Shen, V. Popov

SIMULATED ANGLE DEPENDEND ELECTRON ENERGY DISTRIBUTION

3D - PIC

$N_e (E > 7.5 \text{ MeV}) = 3.3 \times 10^{11} \text{ in } 0.16 \text{ sr,}$



Laser:

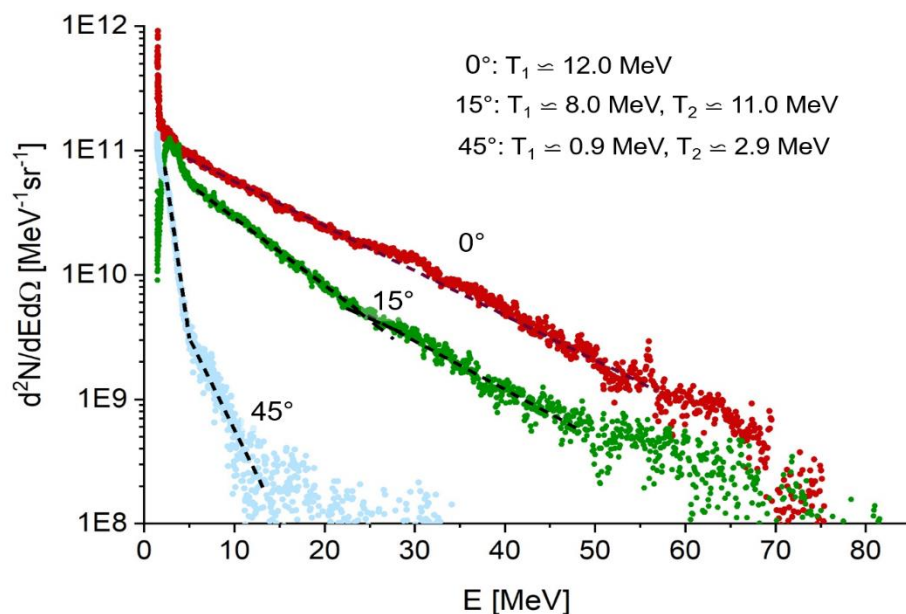
$2.5 \times 10^{19} \text{ Wcm}^{-2}$ ($a_L = 4.28$)

$E_{FWHM} = 17.5 \text{ J}$

$t_{FWHM} = 0.7 \text{ ps}$

Experiment/ foam

$N_e (E > 7.5 \text{ MeV}) = 1.5 \times 10^{11} \text{ in } 0.16 \text{ sr,}$



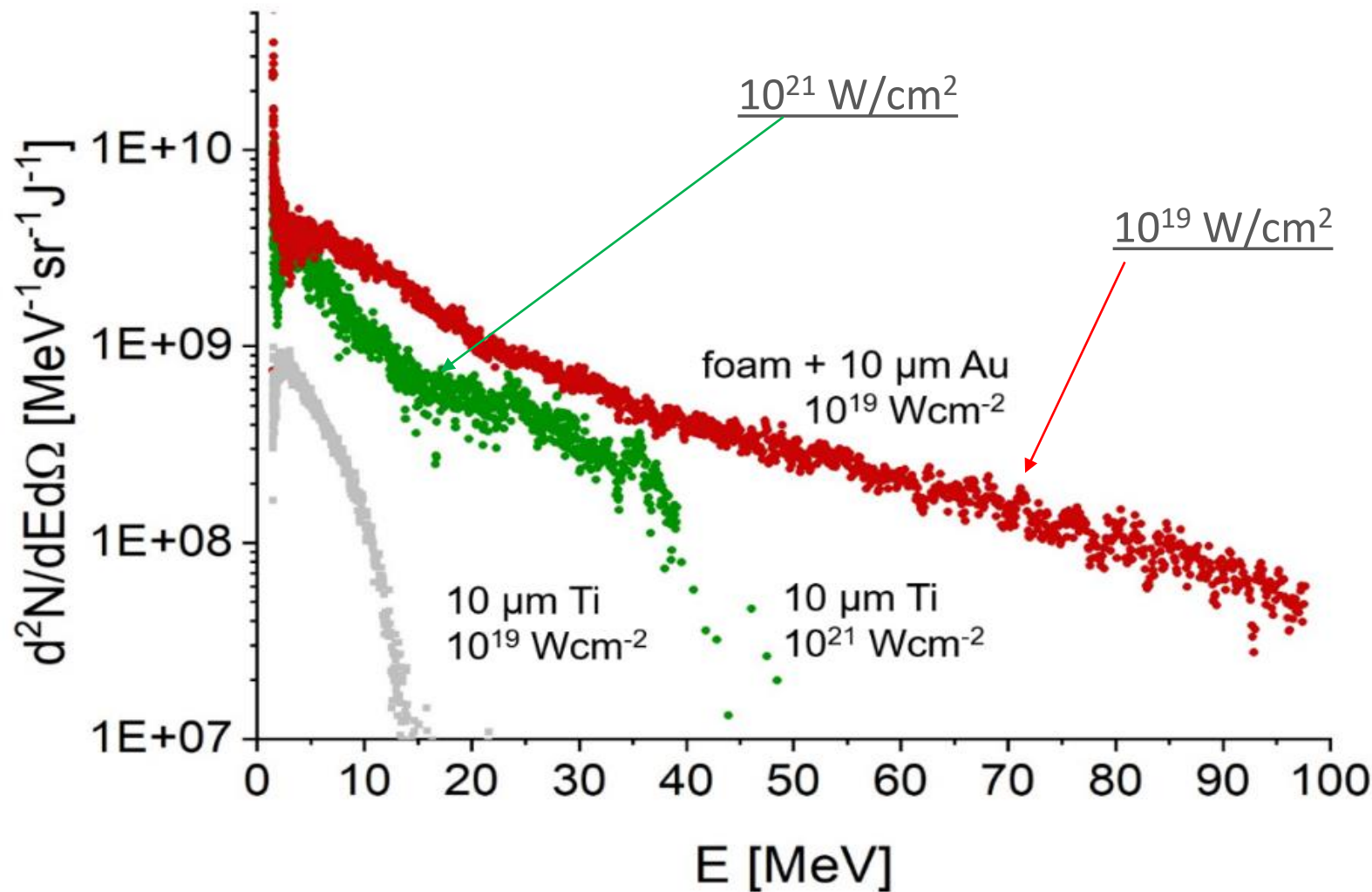
Target:

triacetate cellulose $C_{12}H_{16}O_8$

2 mg/cc $x=300 \mu\text{m}$

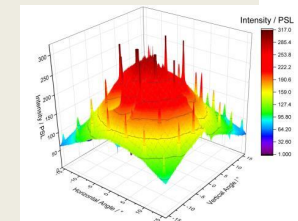
$n_e = 0.65 n_{cr}$ (fully ionized)

ELECTRON ENERGY DISTRIBUTION FOR TWO LASER INTENSITIES



High current, well directed beams of multi-MeV electrons were generated in NCD-plasma at moderate relativistic laser intensities:

- Effective temperature above **10 MeV** (10^{21} W/cm^2 -> foil: 6 -7 MeV)
- Max energy up to **100 MeV** (10^{21} W/cm^2 -> foi: $\sim 40 \text{ MeV}$)
- $E > 3 \text{ MeV}$ propagate in $\frac{1}{2} \theta$ at $\text{FWHM} \leq 13^\circ$
- High current: up to **1 μC** at $E > 2 \text{ MeV}$; $> 50 \text{ nC}$ (6%) $E > 7.5 \text{ MeV}$



Application in Nuclear Physics:

- high fluence/ flux gamma and neutron sources
- high yield (p,xn), (γ,xn) nuclear reactions in Giant Dipole Resonance (GDR) region
- theranostic relevant radio-isotopes.

O N Rosmej et al, New J. Phys. 21(2019) 043044

<https://dx.doi.org/10.1088/1367-2630/ab1047>

“Interaction of relativistically intense laser pulses with long-scale NCD plasmas for optimisation of laser based sources of MeV electrons and gamma-rays”

O. N. Rosmej et al, Plasma Phys. Control. Fusion 62 (2020) 115024

<https://doi.org/10.1088/1361-6587/abb24e>

“High-current laser-driven beams of relativistic electrons for high energy density research”

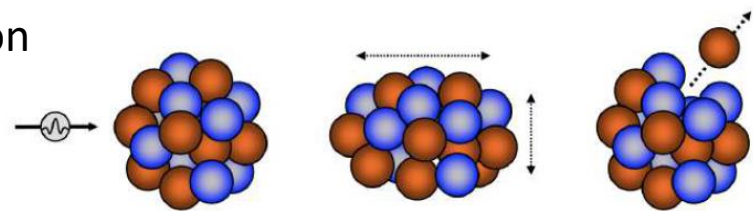
M. M. Guenther et al,

“New insights in laser-generated ultra-intense gamma-ray and neutron sources for nuclear applications and science”

submitted to **Nature Communications**

PHOTO-NUCLEAR REACTIONS

Application of nuclear diagnostics for characterization
of MeV Gamma and neutron beams

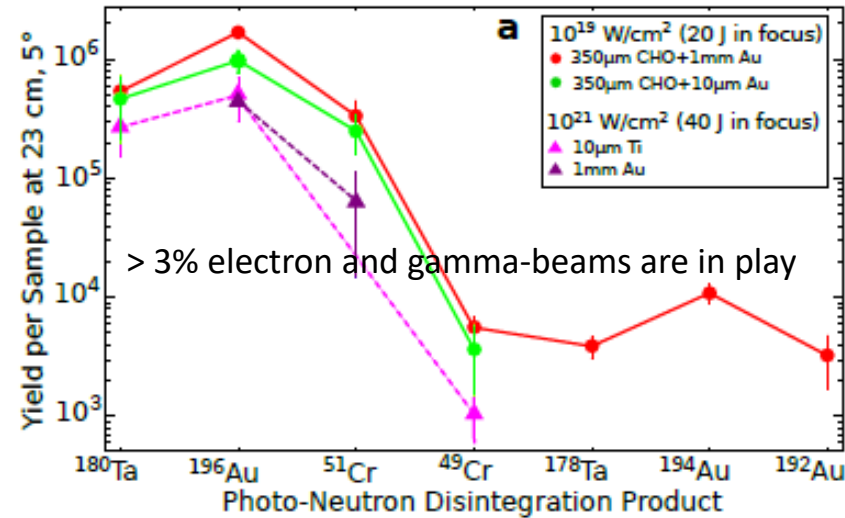
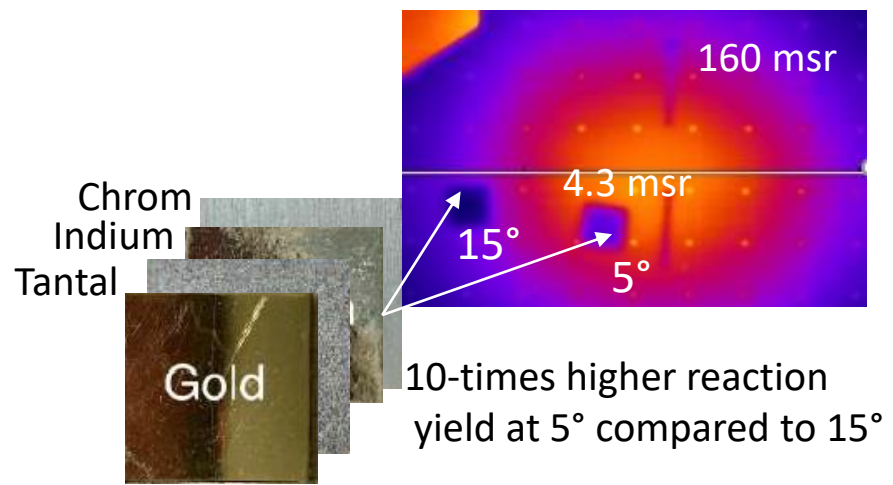


Photodisintegration reactions

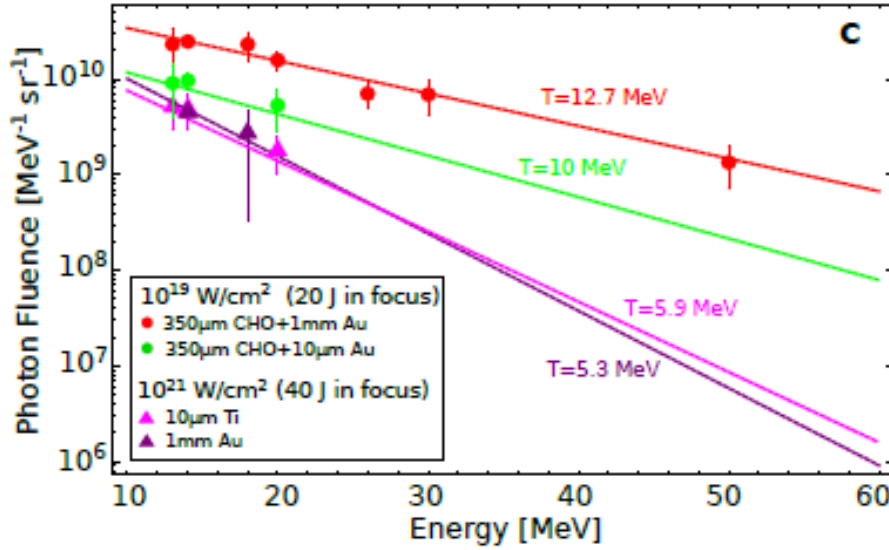
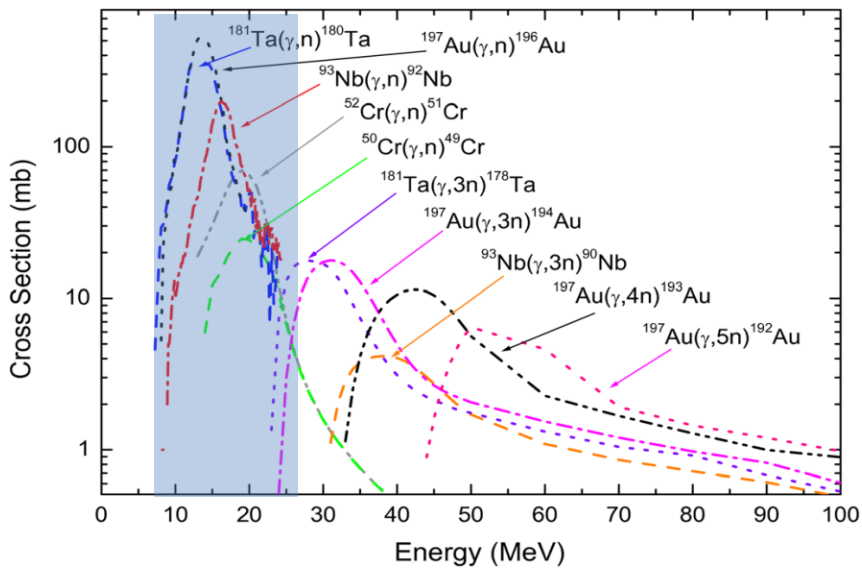
Photonuclear Reaction	Threshold Energy [MeV]	Giant Dipole Resonance (GDR) [MeV]	Half life
$^{181}_{73}Ta(\gamma, n)^{180}_{73}Ta$	7,57	12	8,152 h
$^{197}_{79}Au(\gamma, n)^{196}_{79}Au$	8,03	14	6,183 d
$^{115}_{49}In(\gamma, n)^{114m}_{49}Au$	9,23	15,8	49,5 d
$^{113}_{49}In(\gamma, n)^{112m}_{49}Au$	9,6	15,7	20,56 m
$^{52}_{24}Cr(\gamma, n)^{51}_{24}Cr$	12,04	19	27,7025 d
$^{50}_{24}Cr(\gamma, n)^{49}_{24}Cr$	13	20	42,3 min
$^{115}_{49}In(\gamma, 2n)^{113m}_{24}In$	16,7	19,4	1,6582 h
$^{181}_{73}Ta(\gamma, 3n)^{178m}_{73}Ta$	22,1	28	2,36 h
$^{197}_{79}Au(\gamma, 3n)^{194}_{79}Au$	23,03	32	38,02 h

Günther M M et al 2011 *Phys. Plasmas* **18** 083102

HIGH YIELD OF PHOTO-NUCLEAR REACTIONS

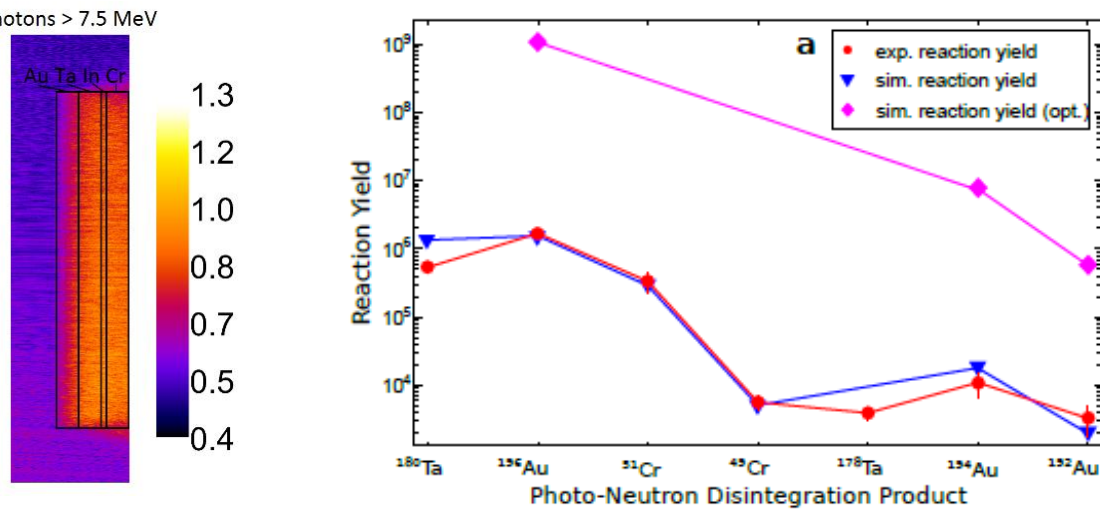
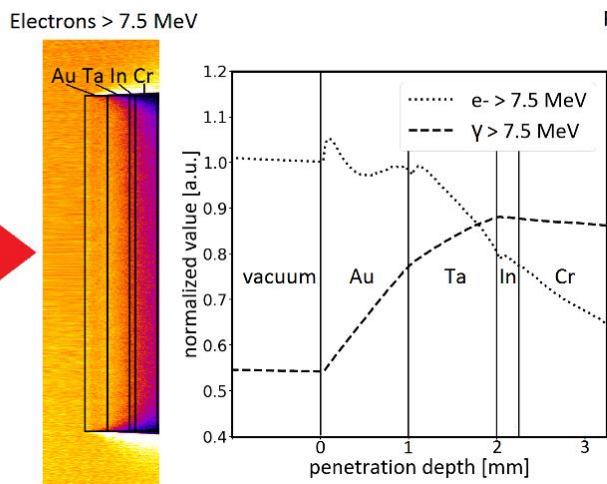
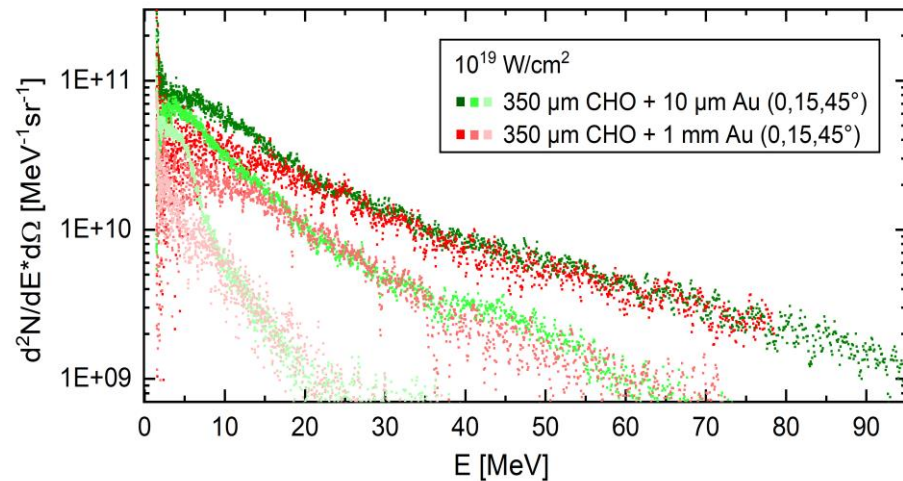
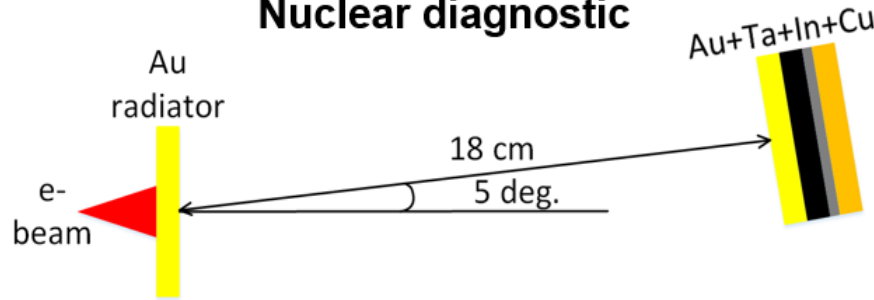


10^{12} ph/sr with $E > 10 \text{ MeV}$ and effective $T=10-13 \text{ MeV}$



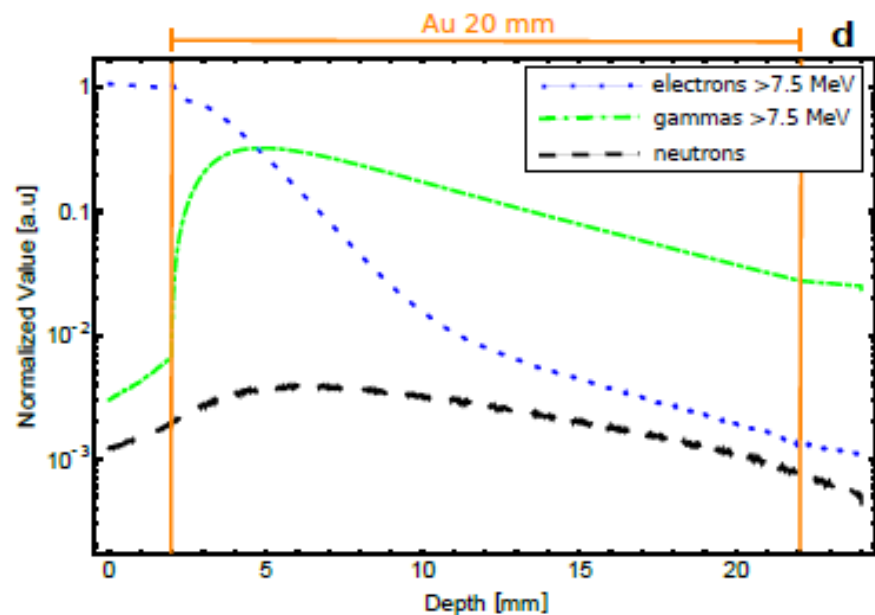
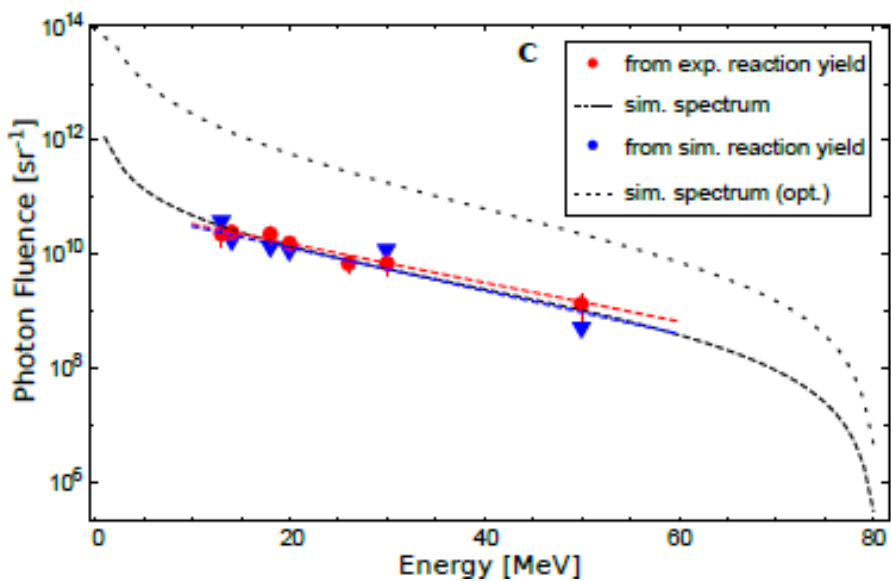
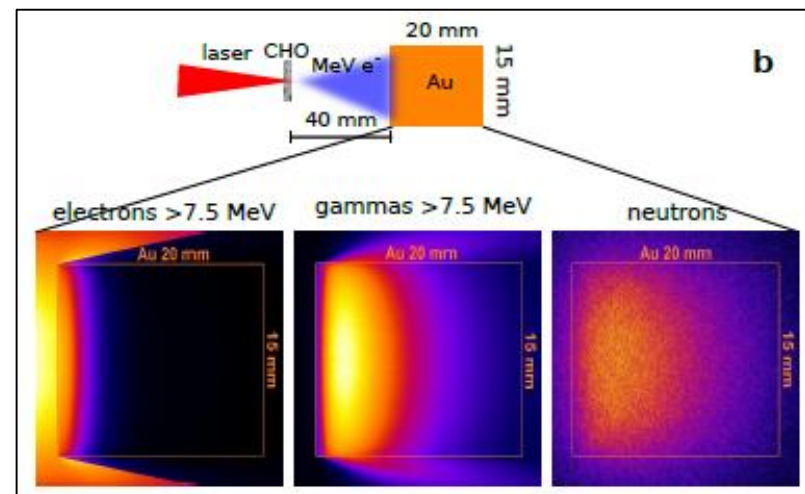
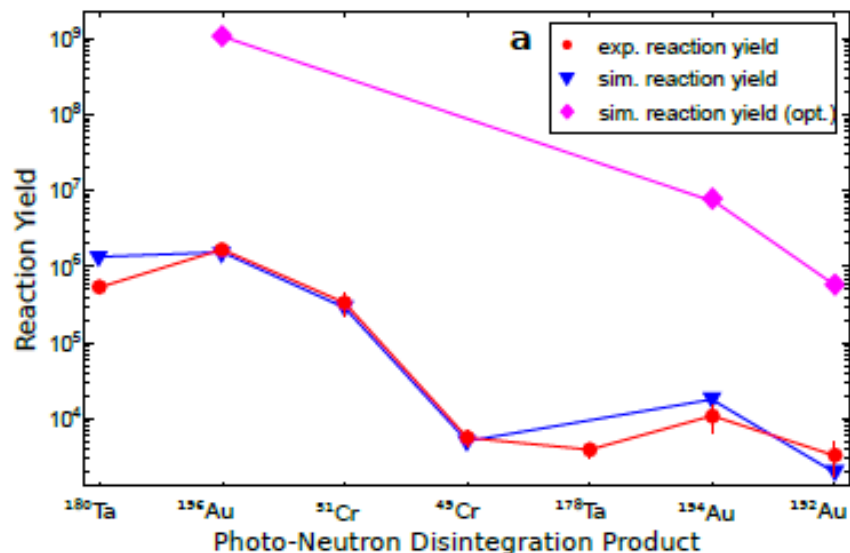
GEANT 4 SIMULATIONS OF REACTION YIELDS

Nuclear diagnostic



A. Skobliakov, ITEP

GEANT4 OPTIMIZATION OF GAMMA AND NEUTRONS PRODUCTION

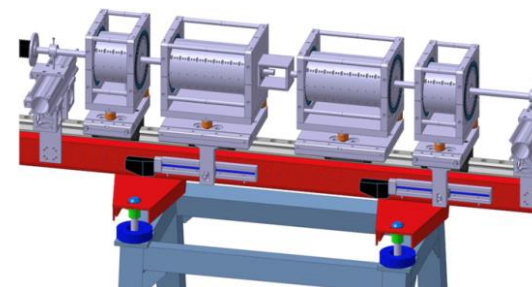
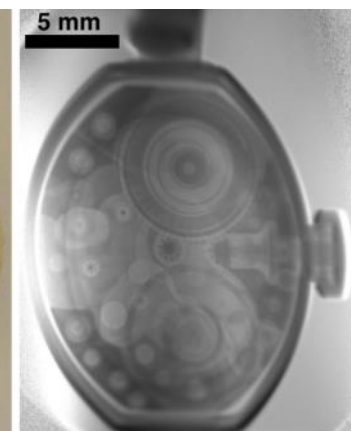


Laser driven X-ray radiography /PHELIX:



Laserpulse: $E=30\text{J}$, $t=700\text{ fs}$, $\text{FWHM}=15\text{ }\mu\text{m}$
Target: $10\text{ }\mu\text{m}$ Au-foil, P176 Sept. 2019

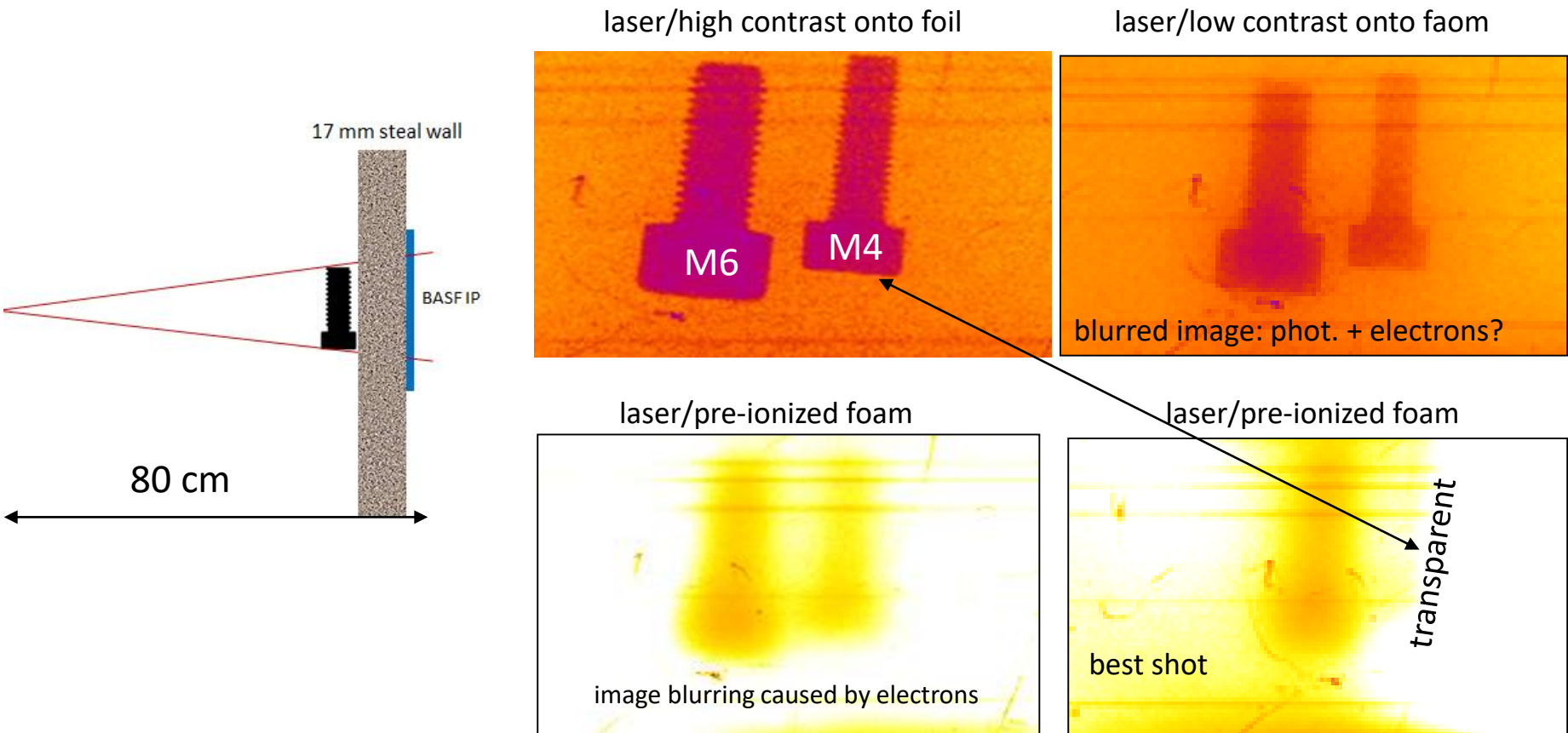
Proton radiography / SIS18



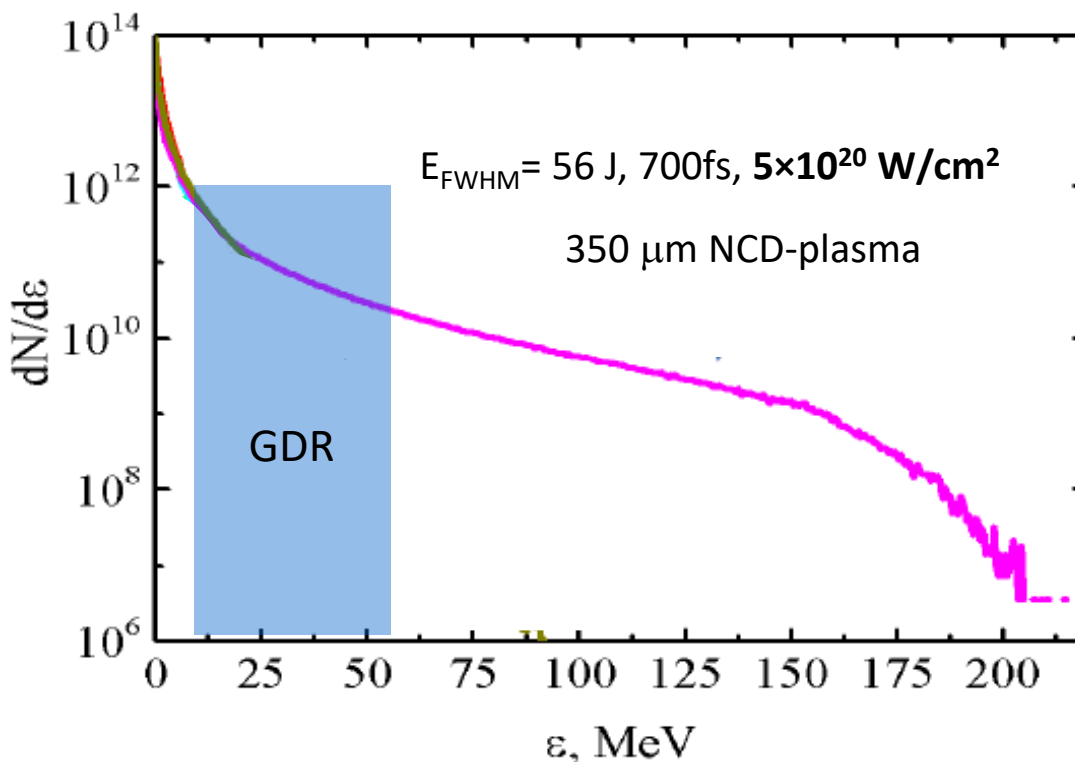
proton microscope for 4 GeV p

GAMMA-RAY RADIOGRAPHY

PHELIX Beam-time 2017



LASER ENERGY OR INTENSITY?



3D PIC,
L. Pugachev,
N. Andreev, JIHT

GEANT- 4 simulations,
A. Skobliakov, ITEP

γ -n reaction yield caused by electrons propagating in $1 \times 1 \times 1 \text{cm}^3$ Au

Isotope (max GDR)	Yield, $5 \times 10^{20} \text{ W/cm}^2$, 60 J	Yield, $2 \times 10^{19} \text{ W/cm}^2$, 20J
196Au (14 MeV)	3,00E+09	1,10E+09
194Au (32 MeV)	4.62E+07	7,62E+06
192Au (50 MeV)	4.44E+06	5,80E+05

25-fold increase of the laser intensity does not lead to much higher reaction yields in the GDR region

INTERNATIONAL COLLABORATION



Theory, simulations: N. E. Andreev, V. Popov (JIHT), X. Shen, A. Pukhov (HHU, Düsseldorf),
A. Skobliakov (ITEP)

Targets: N. G. Borisenko (LPI)

Experiment: M. Guenther, M. Gyrdymov, P. Tavana, S. Zähter, N. Zahn, (GU-Frankfurt),
A. Kantzyrev, V. Panyshkin, A. Skobliakov, A. Bogdanov (ITEP, Moscow),
F. Consoli, M. Salvadori, M. Sciscio (ENEA, Italy),